

UNCLASSIFIED

Defense Technical Information Center
Compilation Part Notice

ADP012539

TITLE: Investigation of the Expansion Rate Scaling of Plasmas in the
Electron Diffusion Gauge Experiment

DISTRIBUTION: Approved for public release, distribution unlimited

This paper is part of the following report:

TITLE: Non-Neutral Plasma Physics 4. Workshop on Non-Neutral Plasmas
[2001] Held in San Diego, California on 30 July-2 August 2001

To order the complete compilation report, use: ADA404831

The component part is provided here to allow users access to individually authored sections
of proceedings, annals, symposia, etc. However, the component should be considered within
the context of the overall compilation report and not as a stand-alone technical report.

The following component part numbers comprise the compilation report:

ADP012489 thru ADP012577

UNCLASSIFIED

Investigation of the Expansion Rate Scaling of Plasmas in the Electron Diffusion Gauge Experiment¹

Kyle A. Morrison, Ronald C. Davidson, Stephen F. Paul, Thomas G. Jenkins

Plasma Physics Laboratory, Princeton University, Princeton, NJ 08543

Abstract. The expansion of the Electron Diffusion Gauge (EDG) pure electron plasma due to collisions with background neutral gas atoms is characterized by the pressure and magnetic field scaling of the profile expansion rate (d/dr) $\langle r^2 \rangle$. Data obtained at higher background gas pressures[1] than previously studied[2] is presented. The measured expansion rate in the higher pressure regime is found to be in good agreement with the classical estimate of the expansion rate[3].

INTRODUCTION

Pure electron plasmas are trapped in the Electron Diffusion Gauge (EDG) device[2, 4, 5, 6], a cylindrically symmetric Malmberg-Penning trap[7] with wall radius $R_w = 2.54$ cm. Previously reported experimental results[2, 6] from the EDG device indicated that the expansion rate of the plasmas is about a factor of four faster than that predicted theoretically. The predicted expansion rate[3] is derived using a fluid treatment of the plasma, and assumes that the (elastic) electron-neutral collision frequency is not a function of time beyond its dependence on the plasma temperature. In this paper, further measurements[1] performed at higher helium background pressures ($P_{He} = 1 \times 10^{-7}$ Torr to 2×10^{-5} Torr) are reported that support the theoretical prediction[3].

Malmberg-Penning traps have a uniform magnetic field parallel to the common axis of several identical cylindrical electrodes, the outer two of which are electrically biased [2, 4, 5, 6, 7]. The EDG device is equipped with a collimating plate and Faraday cup to allow measurements of the plasma's density profile: the particles along an axial chord aligned with the small hole in the collimating plate (the "total" density diagnostic) pass through to the Faraday cup, which measures the amount of charge along that chord (the "local" density diagnostic). By forming several (well-reproduced) plasmas in succession, a series of line-integrated, radial profiles is obtained and used to follow the expansion of the plasma. To determine the plasma behavior at different gas pressures, helium gas is fed into the chamber at different, controlled rates to produce the desired background neutral pressure[2, 4, 5, 6].

¹ Note: Portions of this paper are reprinted from Ref.[1].

EXPANSION RATE MEASUREMENTS

The expansion rate of the plasma in the EDG device is determined as previously described [2, 4, 5, 6]: the mean-square radius of the plasma is computed numerically according to the expression

$$\langle r^2 \rangle = \frac{\int_0^{R_w} dr 2\pi r^2 Q(r)}{\int_0^{R_w} dr 2\pi r Q(r)}, \quad (1)$$

where

$$Q(r) = -\frac{e}{A_h} \int dz \int_{A_h} dr' d\theta n(r', \theta, z). \quad (2)$$

Here, A_h is the area of the collimating hole, and $n(r', \theta, z)$ is the number density of the plasma electrons. The quantity $Q(r)$ corresponds to the axially-integrated profile measured with the local density diagnostic, and is an average over the area of the local density diagnostic's collimating hole (radius = 1/16 in.). The plasma expansion rate may be estimated by fitting a plot of mean-square plasma radius versus time with a curve, and taking the slope of that curve to be the instantaneous expansion rate. In contrast, earlier experiments[8, 9] obtained qualitatively similar scaling results to those presented here with comparable Malmberg-Penning traps by measuring the decay of the plasmas' central density, i.e., both the time it takes for the central density to reach one-half of its initial value, τ_m , and the time rate of change of the inverse central density, $(d/dt)[1/n(r=0, t)]$. For the EDG experiment, however, we have determined the expansion rate from the measured density profiles using a linear fit to the early part of the mean-square radius evolution data.

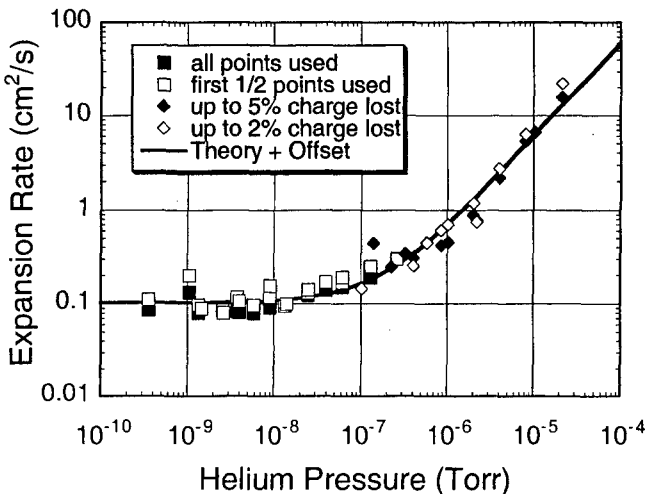


FIGURE 1. The measured plasma expansion rates ($d\langle r^2 \rangle/dt$) at a magnetic field of $B = 610$ Gauss are plotted[1] versus background neutral helium pressure. The squares denote the previous data[2], the diamonds denote the new data[1], and the solid curve is a combination of the theoretical prediction in Eq. (3) plus a constant offset. The plasma line density is $N_L = 3.41 \times 10^7$ electrons/cm.

Figure 1 shows the composite result of the experimental measurements at a $B = 610$ G magnetic field. The data ranging from 3×10^{-10} Torr to 2×10^{-7} Torr, represented by squares, are the data from the previous studies[2, 4, 5, 6]. Each set of mean-square radius data at a particular pressure is represented twice on this plot. Open squares denote the expansion rate determined using only the first half of the mean-square radius evolution data during a four-second time evolution. Closed squares denote the expansion rate determined by using the entire mean-square radius time evolution. Open diamonds denote expansion rates computed using only mean-square radius data taken before 2% of the total plasma charge has been lost, and closed diamonds denote expansion rates computed with the data taken before 5% of the plasma has been lost.

The solid curve in the plot in Fig. 1 is the expansion rate predicted theoretically[3], with an added offset to account for the effects of trap asymmetries[8, 10, 11] at low pressures. The expansion rate in the linear region has previously been calculated[3] to be

$$\frac{d}{dt}\langle r^2 \rangle = \frac{2N_L e^2 v_{en}(T)}{m_e \omega_{ce}^2} \left(1 + \frac{2T}{N_L e^2} \right), \quad (3)$$

where $\omega_{ce} = eB/m_e c$ is the electron cyclotron frequency, $v_{en}(T) = n_n \sigma_{en} v_{Th}$ is the electron-neutral collision frequency, T is the plasma temperature (in ergs), and N_L is the line density of the plasma column. The theoretical curve plotted in Fig. 1 assumes $T = 2$ eV and $N_L = 3.41 \times 10^7$ electrons/cm, and the offset used is $0.1 \text{ cm}^2/\text{sec}$. At pressures exceeding 10^{-7} Torr, the data in Fig. 1 is consistent with the linearly-varying theoretical prediction in Eq. (3). The fit to the data obtained for the previous study[2] resulted in a calculated expansion rate that is factor of four greater than the unadjusted theoretical curve because the data used did not extend to a high enough pressure to produce purely electron-neutral collision-dominated expansion. Note that the theoretical curve plotted in Fig. 1 is not a fit, but an absolute prediction of the fluid theory[3].

In using Eq. (3), however, there is a caveat: at pressures above $P = 10^{-7}$ Torr, the electron-neutral collision frequency in the EDG device is greater than the electron-electron collision frequency [12], and the assumption of uniform temperature across the cross section of the plasma is not necessarily valid. This assumption is used to derive the equation for the expansion rate in Eq. (3), which nonetheless agrees with the measured data. This is interpreted to mean that any effects of a non-uniform plasma temperature on the expansion rate are negligibly small for the EDG device in this parameter range.

Figure 2 shows the results of higher-pressure expansion measurements taken at a $B = 300$ G magnetic field. The squares denote expansion rates computed using the measurements taken before 2% of the plasma has been lost, and the diamonds denote expansion rates computed before 5% of the plasma has been lost. The data used for the expansion rates denoted by triangles is restricted to the profiles in the expansion where low relative error in the computation of $\langle r^2 \rangle$ was obtained. This approximate criterion often results in fewer mean-square radius measurements being used in the computation of the expansion rates than for the 2% case, but in all cases fewer measurements than the number used for the 5% case.

The 300 G data in Fig. 2 also agree with a linear dependence of the expansion rate on background gas pressure. Of the theoretical curves shown, the curve that best describes the linear portion of the data in Fig. 2 is the one that assumes a temperature

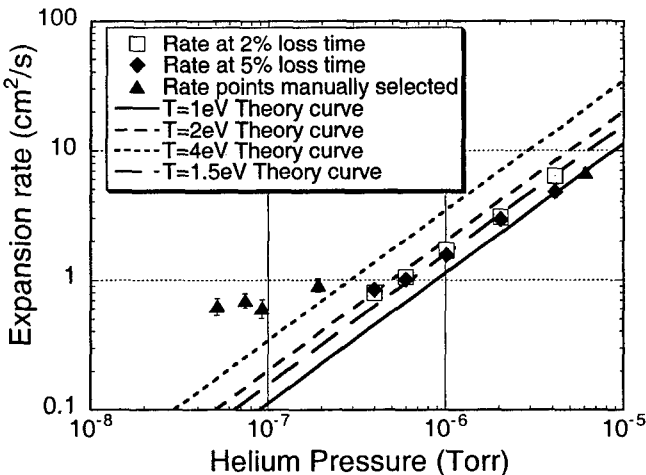


FIGURE 2. The measured plasma expansion rates ($d\langle r^2 \rangle/dt$) at a magnetic field of $B = 300$ Gauss are plotted[1] versus background neutral helium pressure. Theoretical curves for plasma temperatures of $T = 1, 1.5, 2$, and 4 eV are included for comparison. The plasma line density is $N_L = 2.85 \times 10^7$ electrons/cm.

of $T = 1.5$ eV. Plasma temperatures inferred for profiles measured at different times can have different values, however, making it difficult to describe the behavior of the expansion rate with a single theoretical curve.

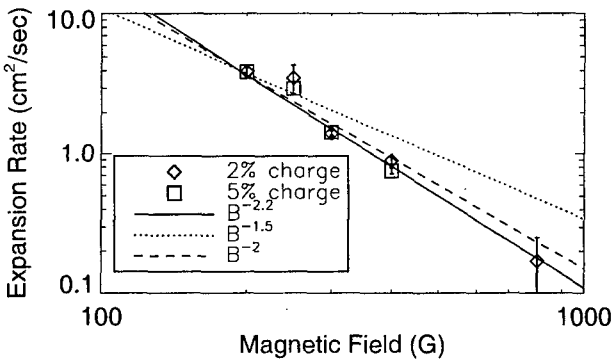


FIGURE 3. The measured plasma expansion rates ($d\langle r^2 \rangle/dt$) are plotted[1] versus magnetic field strength B . The points are best fit by a curve proportional to $B^{-2.19}$. Curves for the lower-pressure scaling[2] of $B^{-1.5}$ and the theoretical scaling B^{-2} are also included.

Expansion rate data has also been taken at $P = 10^{-6}$ Torr at several different values of magnetic field, and the results are presented in Fig. 3. These results indicate that the expansion rate scales as $B^{-2.190 \pm 0.015}$ in the EDG device when electron-neutral collisions dominate the expansion (at higher pressures). The previous (lower-pressure) measurements in the EDG device, in the regime where asymmetry-induced expansion

dominates, produced a scaling of $B^{-1.5 \pm 0.1}$, which is also at variance with the $(L/B)^2$ scaling for that regime reported previously by Driscoll, *et. al*[13, 14]. The measured scaling at higher pressure in the EDG device is in reasonable agreement with the theoretical scaling (B^{-2}) in Eq. (3).

The estimation of the instantaneous expansion rate is complicated by the fact that the temperature changes during the course of the plasma's evolution. In the EDG device, the temperature at a given point in time is routinely inferred by fitting density profile data with the predicted quasi-equilibrium density profile[3]

$$n(r,t) = \hat{n}(t) \exp \left\{ \frac{e\phi(r,t) - e\hat{\phi}(t)}{T} - \frac{r^2}{\langle r^2 \rangle(t)} \left(1 + \frac{N_L e^2}{2T} \right) \right\}, \quad (4)$$

where $\hat{n}(t)$ is the central density as a function of time, $\phi(r,t)$ is the electrostatic potential (the solution of Poisson's equation), and $\hat{\phi}(t)$ is the on-axis electrostatic potential. A Poisson solver routine[15] is used obtain a density profile consistent with both the Boltzmann distribution along the field lines and Poisson's equation. It is important to note that the same fluid theory[3] used to predict the the expansion rate in Eq. (3) is used to predict the quasi-equilibrium density profile in Eq. (4), so the inferred temperatures are imperfect indicators of the actual temperature at pressures above $P = 10^{-7}$ Torr.

Figure 4 shows the temperature evolution at 300 G for background gas pressures of 1×10^{-7} Torr and 1×10^{-6} Torr. In these plots, the black circles are the temperatures determined from the Poisson solver routine, the diamonds are the temperatures determined from fitting the line-integrated profile data directly, and the squares circumscribe points where the inferred Debye length is less than one-fifth of the plasma diameter. The solid curves correspond to the theoretical prediction[16] given the initial conditions, assuming global energy conservation, elastic electron-neutral collisions, and a uniform temperature across the plasma cross-section.

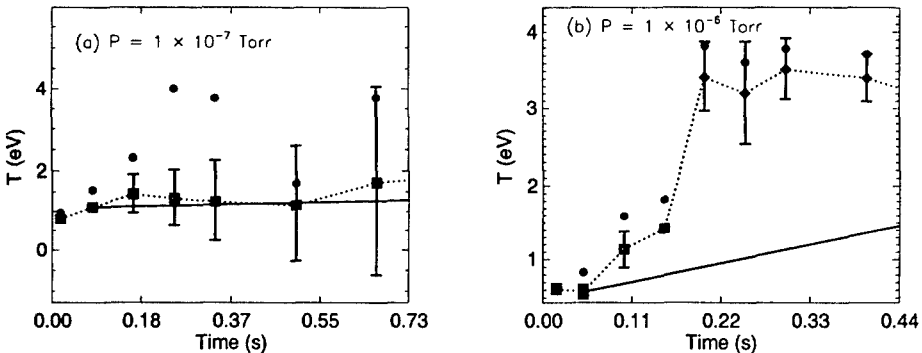


FIGURE 4. These plots display the inferred plasma temperature evolution for the $B = 300$ G data at pressures of 1×10^{-7} Torr and 1×10^{-6} Torr, respectively. The solid line is the theoretical prediction[16]. The dots are obtained from the Poisson solver routine, and the diamonds are obtained from fitting the line-integrated data.

The 10^{-7} Torr data are typical of what was previously measured at lower pressures[2, 4, 5, 6]. The inferred temperatures for the 10^{-6} Torr data after the plasma has lost 2% of the total charge, however, are greater than that predicted theoretically. The reason for the sizeable increase in the inferred temperature in Fig. 4(b) is not understood presently. The plasma is slowly and continuously losing charge throughout the measured density evolution, so wall interactions may be disturbing the evolution of the plasma and forcing it out of the expanding quasi-equilibrium assumed for the temperature inference procedure. It may not be valid to use profile measurements to infer the plasma's temperature under these conditions.

The plasma expansion rate is in good agreement with theoretical predictions[3] at pressures above $\sim 3 \times 10^{-7}$ Torr in the EDG device. The magnetic field scaling of the expansion rate at higher pressures and low rigidity is measured to be proportional to $B^{-2.2}$, in reasonable agreement with the theoretical scaling (B^{-2}) in Eq. (3). Anomalously high temperatures at 1×10^{-6} Torr and 300 G suggest that the plasma may leave its quasi-equilibrium state after the plasma is in good contact with the trap wall.

ACKNOWLEDGMENTS

This research was supported by the Office of Naval Research.

REFERENCES

1. K. A. Morrison, R. C. Davidson, S. F. Paul, E. A. Belli, and E. H. Chao, *Phys. Plasmas* **8**, 3506 (2001).
2. E. H. Chao, R. C. Davidson, S. F. Paul, and K. A. Morrison, *Phys. Plasmas* **7**, 831 (2000).
3. R. C. Davidson and D. A. Moore, *Phys. Plasmas* **3**, 218 (1996).
4. E. H. Chao, S. F. Paul and R. C. Davidson, *J. Vac. Sci. Technol. A* **17**, 2034 (1999).
5. E. H. Chao, R. C. Davidson and S. F. Paul, *J. Vac. Sci. Technol. A* **17**, 2050 (1999).
6. E. H. Chao, R. C. Davidson, S. F. Paul, and K. A. Morrison, *Proceedings of the 1999 Workshop on Nonneutral Plasmas* (Princeton University, 1999); American Institute of Physics Conference Proceedings, No. 498, edited by J. Bollinger, R. C. Davidson, and R. Spencer (American Institute of Physics, Melville, NY, 1999), p. 278.
7. J. S. deGrassie and J. H. Malmberg, *Phys. Rev. Lett.* **39**, 1077 (1977).
8. J. H. Malmberg and C. F. Driscoll, *Phys. Rev. Lett.* **44**, 654 (1980).
9. J. S. deGrassie and J. H. Malmberg, *Phys. Fluids* **23**, 63 (1980).
10. J. M. Kriesel and C. F. Driscoll, *Phys. Rev. Lett.* **85**, 2510 (2000).
11. J. Notte and J. Fajans, *Phys. Plasmas* **1**, 1123 (1994).
12. E. H. Chao, Ph.D. Thesis, Princeton University (1999).
13. C. F. Driscoll and J. H. Malmberg, *Phys. Rev. Lett.* **50**, 167 (1983).
14. C. F. Driscoll, K. S. Fine and J. H. Malmberg, *Phys. Fluids* **29**, 2015 (1986).
15. E. H. Chao, R. C. Davidson, S. F. Paul, and K. S. Fine, *Proceedings of the 1999 Workshop on Nonneutral Plasmas* (Princeton University, 1999); American Institute of Physics Conference Proceedings, No. 498, edited by J. Bollinger, R. C. Davidson, and R. Spencer (American Institute of Physics, Melville, NY, 1999), p. 461.
16. R. C. Davidson and E. H. Chao, *Phys. Plasmas* **3**, 2615 (1996).